Endometrial luminal epithelial cells sense embryo elongation in the roe deer independent of interferon-tau†

Authors: van der Weijden, Vera A., Puntar, Brina, Vegas, Alba Rudolf, Milojevic, Vladimir, Schanzenbach, Corina I., et al.

OXFORD

Research Article

Endometrial luminal epithelial cells sense embryo elongation in the roe deer independent of interferon-tau[†]

**Vera A. van der Weijden[1], Brina Puntar[1], Alba Rudolf Vegas[1],
Vladimir Milojevic[1], Corina I. Schanzenbach[1], Mariusz P. Kowalewski[2],
Barbara Drews[1] and Susanne E. Ulbrich[1,*]**

[1]ETH Zurich, Animal Physiology, Institute of Agricultural Sciences, Zurich, Switzerland, and [2]Institute of Veterinary Anatomy, Vetsuisse Faculty, University of Zurich, Zurich, Switzerland

*Correspondence: ETH Zurich, Animal Physiology, Institute of Agricultural Sciences, Zurich, Switzerland.
Tel: +41446322721; E-mail: susanne.ulbrich@usys.ethz.ch

Abstract

Numerous intrauterine changes take place across species during embryo development. Following fertilization in July/August, the European roe deer (*Capreolus capreolus*) embryo undergoes diapause until embryonic elongation in December/January. Embryonic elongation prior to implantation is a common feature among ungulates. Unlike many other ruminants, the roe deer embryo does not secrete interferon-tau (IFNτ). This provides the unique opportunity to unravel IFNτ-independent signaling pathways associated with maternal recognition of pregnancy (MRP). This study aimed at identifying the cell-type–specific endometrial gene expression changes associated with the MRP at the time of embryo elongation that are independent of IFNτ in roe deer. The messenger RNA (mRNA) expression of genes known to be involved in embryo–maternal communication in cattle, pig, sheep, and mice was analyzed in laser capture microdissected (LMD) endometrial luminal, glandular epithelial, as well as stromal cells. The mRNA transcript abundances of the estrogen (*ESR1*), progesterone receptor (*PGR*), and IFNτ-stimulated genes were lower in the luminal epithelium in the presence of an elongated embryo compared to diapause. Retinol Binding Protein-4 (*RBP4*), a key factor involved in placentation, was more abundant in the luminal epithelium in the presence of an elongated embryo. The progesterone receptor localization was visualized by immunohistochemistry, showing an absence in the luminal epithelium and an overall lower abundance with time and thus prolonged progesterone exposure. Our data show a developmental stage-specific mRNA expression pattern in the luminal epithelium, indicating that these cells sense the presence of an elongated embryo in an IFNτ-independent manner.

Summary Sentence

Cell-type–specific gene expression analysis shows that luminal epithelium cells sense embryo elongation in the roe deer.

Key words: diapause, endometrium, preimplantation embryo

Introduction

Adequate embryonic developmental-stage specific interactions with the endometrium are required to allow successful embryo implantation [1]. Around the time of elongation, physical and chemical properties of the embryo enable an appropriate maternal recognition of pregnancy (MRP). Depending on the species, the MRP is an antiluteolytic or luteotropic mechanism that facilitates the transition from cyclicity to pregnancy, and thus is essential for the maintenance of pregnancy. In cattle and sheep, interferon-tau (IFNτ) is the major MRP signal, while in pigs, estrogens have most prominently been reported [1]. The perception of the MRP signal results in numerous differentially expressed genes (DEG) in a cell-type–specific manner in the endometrium [2, 3].

The endometrium in ruminants consists of intercaruncular (*icar*) endometrium and the caruncles (*car*). The *icar* is mainly involved in adapting the microenvironment to the needs of the preimplantation embryo through its secretory activity via endometrial glands, while the *car* constitute the site of later placentation [4]. The *icar* endometrium consists of the luminal epithelium (LE), glandular epithelium (GE), and the stroma (STR), whereas the *car* endometrium is devoid of glands [4]. During preimplantation embryo development, ovarian progesterone (P4) stimulates the secretory function of the endometrial LE and GE. Although the P4 concentration remains high during the luteal phase and early pregnancy in ruminants [5–7], the LE and GE gradually loose the expression of the progesterone receptor (PR) from days 12 to 14 onward during both the normal cycle and pregnancy [5–7]. Upon loss of the PR in the LE and GE, P4 is known to act indirectly via PR expressed on stromal cells and the induction of progestamedins [8]. The function of P4 is essential for successful embryo development and implantation [9]. Irrespective of the species-specific MRP signal, endometrial cell-type–specific gene expression changes have been observed in various species. In the preimplantation mouse endometrium, the LE predominantly expressed lipid-, metal-ion binding-, and carbohydrate-related genes, whereas the GE showed highest gene expression of immune response genes [2]. During the preimplantation phase in sheep, the dynamic gene expression changes in LE and GE underline the importance of investigating MRP as such, and its cell-type–specific perception [3]. The number of expressed genes increased between days 10 and 20 in the LE, whereas the GE showed an increase in the number of expressed genes from day 10 to 14, which decreased from days 14 to 20 [3]. In pregnant sheep, genes involved in cell survival and growth were expressed from days 10 to 14, and genes involved in cell organization and protein synthesis were expressed from days 16 to 20 [3].

Like in other ungulates, the embryo of the European roe deer (*Capreolus capreolus*) rapidly elongates prior to implantation. Yet, this only occurs after an obligatory 4-month developmental delay, known as embryonic diapause [10]. Embryonic diapause has been described in over 130 species across several different orders of eutheria [11]. It occurs either obligatory or facultative, is driven by several species-specific stimuli, and the duration ranges from several days to months. The roe deer is the only known ungulate that displays embryonic diapause. Changes between diapause and embryo elongation in uterine fluid constituents have been described, i.e., a rise in hexose, fructose, total protein, α-amino nitrogen, and calcium [12–14]. The corpus luteum remains active during the entire period of embryonic diapause and embryo elongation. We recently focused on P4 secretion specifically during reactivation and did not find any indication thereof [15]. By using

a holistic proteomics approach, we have previously shown that the roe deer embryo at diapause faces an environment with high cellular detoxification, and that there is an increased abundance of proliferation-inducing proteins at elongation [16]. During embryo reactivation, no concentration changes have been shown for classical ungulate embryonic MRP signals such as IFNτ, estrogens, or chorionic gonadotropins, and for the maternal signals for embryo reactivation such as prolactin, P4, and estrogens [12–15, 17–19].

To date, the understanding of the regulation of diapause and embryo elongation in roe deer is still limited. It has previously been shown that maternal serum pregnancy-associated glycoproteins (PAG) levels increased after embryo elongation, which was hypothesized to facilitate embryo implantation and was found to cause an increase in maternal 17β-estradiol [17]. We aimed at shedding light on embryo–maternal interactions in roe deer by providing a first insight into endometrial cell-type–specific gene expression changes between diapause and elongation. The roe deer is the only ruminant known not to signal pregnancy via IFNτ [19]. Thus, it serves as model species for ruminants that allows to perceive MRP signaling independent of IFNτ. Thirty-one target genes that have previously been shown to be implicated in the embryo–maternal interaction around the time of embryo elongation in cattle, sheep, pigs, and mice were selected for cell-type–specific mRNA gene expression analyses. The target genes included oxytocin receptor (OXTR), fibroblast growth factor 1 (FGF1), aromatase (CYP19A1), cytochrome P450 family 1 subfamily B member 1 (CYP1B1), cytochrome P450 family 1 subfamily A member 1 (CYP1A1), aldo-keto reductase family 1 member B (AKR1B1), interferon regulatory factor 2 (IRF2), ISG15 ubiquitin like modifier (ISG15), MX dynamin like GTPase 1 (MX1), hydroxysteroid 11-beta dehydrogenase 1 (HSD11B1), carbonyl reductase 1 (CBR1), prostaglandin E synthase (PTGES), prostaglandin E receptor 2 (PTGER2), solute carrier family 1 member 5 (SLC1A5), solute carrier family 2 member 1 (SLC2A1), solute carrier family 5 member 1 (SLC5A1), solute carrier family 15 member 3 (SLC15A3), estrogen receptor 1 (ESR1), progesterone receptor (PGR), H3 histone, family 3A (H3F3A), tyrosine 3-monooxygenase/tryptophan 5-monooxygenase activation protein zeta (YWHAZ), glyceraldehyde-3-phosphate dehydrogenase (GAPDH), vascular endothelial growth factor A (VEGFA), fibroblast growth factor receptor 1 (FGFR1), fibroblast growth factor receptor 2 (FGFR2), TIMP metallopeptidase inhibitor 2 (TIMP2), matrix metallopeptidase 14 (MMP14), matrix metallopeptidase 9 (MMP9), retinol binding protein 4 (RBP4), secreted protein acidic and cysteine rich (SPARC), and heparin binding EGF like growth factor (HBEGF). In this study, we aimed at identifying transcriptional changes associated with the MRP at the time of embryo elongation that are independent of IFNτ in roe deer.

Materials and methods

Sample collection

Roe deer tissue samples (*n* = 81) were obtained in the course of regular huntings in Switzerland between September and December 2016. Ethical approval was neither required nor available as field sampling was performed from regular huntings, where animals were shot for hunting purposes. Within 2–4 h after the animal was shot, the uterus was collected and the embryos were recovered by uterine flushing with 2.5-ml Phosphate-buffered saline (PBS) and their diameters were determined using a Zeiss SteREO Discovery.V8 microscope, an Olympus SC50 camera, and CellSens software. Approximately

100 mg of tissue samples from *car* and *icar* endometrium were collected from each animal, and samples were snap frozen in liquid nitrogen and conserved at −80 °C after maximally 8 h after the animal was shot. The uterine fluid was centrifuged for 10 min at 800× g at 4 °C. The supernatant was snap frozen in liquid nitrogen and stored at −80 °C. For the mRNA expression analysis, animals were randomly selected based on sampling date and a comparable, mean embryo size. To represent the blastocysts, three animals sampled between 29.10.2016 and 08.11.2016 with embryo sizes of 0.84 ± 0.17 mm (mean ± SEM) were selected, and for the elongated embryos, four animals sampled between 02.12.2016 and 28.12.2016 with embryo sizes of 47.14 ± 6.23 (mean ± SEM) were selected. Nineteen uteri collected between September 10 and December 28 covering the different developmental stages, i.e., a blastocyst at diapause and elongated embryos following diapause, were stained against the PR.

Interferon-tau quantification

IFNτ protein was analyzed using an in-house established sandwich ELISA against bovine IFNτ [20]. According to a blast of the bovine genome and roe deer transcriptome, the sequence similarity is about 78%. The deduced protein similarity of the roe deer IFNτ sequence showed between 71 and 78% similarity to bovine. The detection limit of the ELISA was 13 pg/ml. The assay did not cross-react against related bovine interferons (IFNα, IFNβ, and IFNγ), except for a 4% cross-reactivity against the closest IFNτ relative IFNω [20]. IFNτ was measured in duplicates in 1–10 µl of roe deer uterine fluid [20].

Laser capture microdissection

Cryosections were prepared for each tissue piece with a Leica CM 1950 Cryotome. Each tissue piece was embedded in optimal cutting temperature compound (OCT compound) (Biosystems, cat. # 3801480S), and sections of 10 µm thickness were cut at a temperature of −25 °C for the cryo chamber and −20 °C for the specimen head. Sections were mounted on 1.0 PEN NF Membrane Slides (Zeiss, cat. # 415190-9081-000) and stained with 1% (w/v) cresyl violet acetate (Sigma Aldrich, cat. # 86098-0) in 50% EtOH. The membrane slide with mounted sections was placed in 70% EtOH for 3 min, dipped twice into 50% EtOH, stained with cresyl violet for 2 min, dipped twice into 50% EtOH, dipped twice into 70% EtOH, dipped twice into 100% EtOH, followed by air-drying at room temperature for 3 min. The stained sections were stored at −80 °C until further processing. The LE, GE, and STR were dissected from the *icar* endometrium, and the LE and STR were dissected from the *car* endometrium. To that end, the Carl Zeiss inverse microscope with Excite metal-halide lamp, AxioCam Mrm camera, 355-nm pulsed UV laser, and PALM Robo Release 4.3 Software was used. Approximately 100 pieces of each selected cell type were collected in separate adhesive caps (Zeiss, cat. # 415190-9191-000). All laser capture micro-dissected (LMD) samples were stored at −80 °C until nucleic acid isolation.

Nucleic acid isolation

Total RNA and DNA were isolated from the LMD samples using the AllPrep DNA/RNA Micro Kit (Qiagen, Hilden, Germany), according to the manufacturer's instructions for isolation of LMD samples. The samples were lysed in 350 µl of RLT Plus buffer, and total RNA was isolated by adding 350 µl of 100% ethanol to the DNA spin column flow-though. RNA was eluted in a volume of 12 µl RNase-free water. After the isolation, the RNA integrity was determined with the Agilent 2100 Bioanalyzer RNA 6000 Pico kit (Agilent, cat. # G2939A), according to the Agilent RNA 600 Pico Kit Quick Start guide instructions. The samples displayed an RNA integrity of 7.6 ± 0.6 (mean ± SD). The DNA concentration was quantified by using 10 µl of DNA with the Promega Quantus Fluorometer and the Promega QuantiFluor ONE dsDNA System (Promega, cat. # E4871), according to manufacturers' instructions.

Target gene selection

The target gene selection was based on a priori functional knowledge of specific genes in embryo–maternal communication and the maternal response to embryo elongation in cattle, pig, sheep, and mice. A PubMed database search with the following keywords was conducted: "embryo–maternal communication," "embryo elongation," "gene expression," "transcriptomics," "cattle," "pig," "sheep," and "mice." A set of 31 target genes was selected for the gene expression analysis. The target genes were subdivided into five functional categories, i.e., "steroidogenesis and hormone receptors," "IFN-stimulated genes," "prostaglandin synthesis and receptors," "transporters," and "proliferation and tissue remodeling."

Primer design

Primers were designed for amplification of 31 roe deer–specific mRNA sequences. Conserved regions of *Bos taurus*, *Equus caballus*, *Sus scrofa*, *Homo sapiens*, *Mus musculus,* and *Ovis aries* were identified and selected using the Align Nucleotide Blast in the NCBI database. Given the relatively high evolutionary similarity between roe deer and cattle, the primer sequence was deduced from the *Bos taurus* sequence. The amplicons were sequenced and used for roe deer–specific primer design. Primers were designed with the NCBI Primer BLAST tool, and oligonucleotides were ordered from Microsynth (Balgach, Switzerland). The specificity of the primers was confirmed by gel electrophoresis and melting curve analysis within the Bio-Rad CFX Manager 30 software. The primer pair specifications can be found in Supplementary Table 1.

Specific target amplification and real-time quantitative polymerase chain reaction

Due to the limited amount of available RNA for a downstream analysis, the total DNA was used to normalize the RNA input for the specific target amplification (STA) and subsequent polymerase chain reaction (PCR) (a high correlation was found between DNA and RNA concentration, and therefore this approach was considered as adequate). The CellsDirect One-Step qRT-PCR Kit (ThermoFisher Scientific, Waltham, MA, USA, cat. # 11753100) was used for target-specific cDNA synthesis and STA, as described previously [21], with minor modifications. The STA master mix was prepared by mixing 5 µl 2× Reaction Mix, 0.2 µl CellsDirect Enzyme Mix, 2.5 µl primer mix, 0.2 µl SUPERase● In RNase Inhibitor (20 U/µl) (ThermoFisher Scientific, Waltham, MA, USA, cat. # AM2694), and 1× TE buffer (ThermoFisher Scientific, Waltham, MA, USA, cat. # 12090015). Two microliters of equal amounts of RNA, corresponding to an input of 4.7 pg of DNA, were mixed with 8 µl of STA master mix. Reverse transcription was performed in a thermal cycler by incubation for 15 min at 50 °C, followed by 2 min incubation at 95 °C. Directly following reverse transcription, the STA was performed in a thermal cycler by 18 cycles of 15 s at 95 °C and 4 min at 60 °C. All the reactions were cleaned up from residual single-stranded DNA by treatment with an Exonuclease I master mix containing 0.8 µl Exonuclease I (20 U/µl) (ThermoFisher Scientific, Waltham, MA,

USA, cat. # EN0581), 0.4 µl 10× Exonuclease I Reaction Buffer, and 2.8 µl nuclease-free water. The STA product was supplemented with 4 µl of Exonuclease I master mix and incubated at 37 °C for 15 min, followed by heat inactivation of the enzyme at 80 °C for 15 min. The cleaned-up STA samples were used for gene expression analysis using a Biomark HD instrument according to manufacturers' instructions and as described previously [22]. The Sample Pre-Mix, containing 3 µl 2× TaqMan Gene Expression Master Mix (Applied Biosystems, Foster City, CA, USA, cat. # PN 4369016), 0.3 µl 20× DNA Binding Dye Sample Loading Reagent (Fluidigm, San Francisco, CA, USA, cat. # PN 100–0388), 0.3 µl 20× EvaGreen DNA binding dye (Biotium, Fremont, CA, USA, cat. # PN 31000), and 0.9 µl TE buffer, was combined with 1.5 µl of 10× diluted cleaned-up STA cDNA. The Assay Mix was prepared for 48 primer pairs, containing 3 µl 2× Assay Loading Reagent (Fluidigm, San Francisco, CA, USA, cat. # PN 85000736), 0.3 µl TE buffer, and 2.7 µl 20 µM of Forward and Reverse Primer Mix. The 48.48 Dynamic Array (Fluidigm, San Francisco, CA, USA, cat. # BMK-M-48.48) chip was loaded and run as described in the Fluidigm Advanced Development Protocol 14. After a hot start of 120 s at 50 °C and 600 s at 95 °C, the amplification was performed by 40 cycles of 15 s at 95 °C and 60 s at 60 °C. A melting curve was generated by a temperature increase from 60 to 95 °C with increments of 1 °C/s.

Progesterone receptor localization

Immunohistochemistry was performed with an indirect immunoperoxidase method [23, 24]. Tissue samples were formalin fixed, paraffin embedded, cut at 2–3 µm, dewaxed in xylol, and rehydrated in graded ethanol series. Antigen retrieval was performed with 10-mM citrate buffer at pH 6.0 in a microwave oven at 560 W for 15 min. Endogenous peroxidase was quenched with 0.3% H_2O_2 in methanol for 30 min. The following buffer was used for equilibrating tissue sections: 0.8 mM Na_2HPO_4, 1.47 mM KH_2PO_4, 2.68 mM KCl, 137 mM NaCl, and 0.3% Triton X, at pH 7.2–7.4. Nonspecific binding sites were blocked with 10% horse serum for 20 min at ambient temperature. The primary antibody was the mouse mAb against the human C-terminal PGR, clone 10A9, Immunotech, Hamburg, Germany (dilution 1:20), and the irrelevant mouse IgG (Vector Laboratories Vector Laboratories Inc., Burlingame, CA, USA) was used as isotype control (negative control) in the same protein concentration as the primary antibody. Antibodies were applied and incubated overnight at 4 °C. An additional negative control was included by omitting the primary antibody. The secondary antibody was the horse antimouse IgG BA-2000 (Vector Laboratories), which was 1:100 diluted, and samples were incubated for 30 min at ambient temperature. Signals were enhanced with the streptavidin-avidin-peroxidase Vectastain ABC kit (Vector Laboratories), for 30 min at ambient temperature. Signals were detected with DAB+ substrate kit (Dako Schweiz, AG). Sections were counterstained with hematoxylin. The localization of PR staining was assessed and scored according to the staining intensity as "negative," "weak/sporadic," "medium," and "strong" in a blinded manner.

Data analysis

The Fluidigm Real-Time PCR Analysis Software was used for the quality control of the experiment and for product specificity validation. To allow for the analysis of genes with very low mRNA expression, a cut-off value of cycle of quantification (Cq) = 24 was set as limit of detection, and a Cq of 24 was assigned to genes where the expression was lower. The "bestkeeper" was calculated as geo-

metrical mean of the Cq values of *GAPDH*, *H3F3A*, and *YWHAZ* and was found to be the most stable reference gene according to the geNorm algorithm in the GenEx6 software [25]. All data were normalized by calculating the ΔCq as $Cq_{reference} - Cq_{target}$ plus an arbitrary unit of 15 to display positive digits. The mean expression values ± standard deviation can be found in Supplementary Table 2. The normalized expression values were $\log_2$ transformed, centered and a PCA plot and a heatmap were generated in R Studio [26]. The statistical analysis to identify DEG between the blastocyst and elongated stage within one specific cell type was performed on ΔCq values in IBM SPSS Statistics 23 using a *T*-test. Graphs of DEG were made in GraphPad Prism 7.02.

Results

Lack of interferon-tau signaling by the developing embryo

The roe deer uterine fluid IFNτ concentration was lower than the limit of detection (13 pg/ml) at both developmental stages (data not shown).

Cell-type–specific mRNA expression during embryo development

The different analyzed cell types are shown in Figure 1A. The heatmap (Figure 1B) based on fold changes between the two developmental stages (*n* = 3 for the blastocyst stage at diapause and *n* = 4 for the elongated embryos following diapause) showed a difference between the LE in both *icar* and *car* and the other cell types. The *icar* and *car* from whole tissue cluster together, and their expression pattern was largely similar to the *icar* and *car* STR and the *icar* GE. The DEG largely overlapped in the *icar* and *car* LE. The *icar* from the whole tissue uniquely showed differential expression of *FGF1*, *MMP14*, and *MMP9*. In addition, the *icar* STR was the only cell type displaying differential gene expression of *SPARC* and of *TIMP2*.

As shown in the PCA plot (Figure 1C), the cell-type–specific mRNA expression is apparent in the clear separation of different cell types. Irrespective of the developmental stage, the *icar* and *car* STR and the *icar* GE formed separate clusters. A developmental-stage dependent separation for both *car* and *icar* LE was observed. While nine DEG appeared in both *icar* and *car* LE, a lower expression of *ESR1* and *AKR1B1* was specific to the *icar* LE upon elongation, and a lower expression of *CYP19A*, *PTGES*, and *ISG15*, and a higher expression of *CYP1A1* was specific to the *car* LE upon elongation (Figure 1D).

DEG were evident in different functional categories, i.e., *HSD11B1, CYP19A, CYP1A1, CYP1B1, PGR*, and *ESR1* in the category "Steroidogenesis and hormone receptors"; *IRF2, MX1*, and *ISG15* in the category "IFN-stimulated genes"; *AKR1B1* and *PTGES* in the category "prostaglandin synthesis and receptors"; *SLC15A3* and *SLC5A1* in the category "transporters"; and *RBP4* and *FGFR2* in the category "proliferation and tissue remodeling." Contrary to the LE, there were only two DEG in the *icar* GE (*SLC15A3* and *TIMP2*) and one DEG in the *icar* STR (*SPARC*).

Developmental-stage–specific mRNA expression in the luminal epithelium

In the *icar* LE, genes involved in "steroidogenesis and hormone synthesis," i.e., *HSD11B1*, *CYP1B1*, *PGR*, and *ESR1*, displayed a developmental-specific expression (Figure 2). *HSD11B1* showed a 12.4-fold higher expression, whereas *CYP1B1* showed a 4.1-
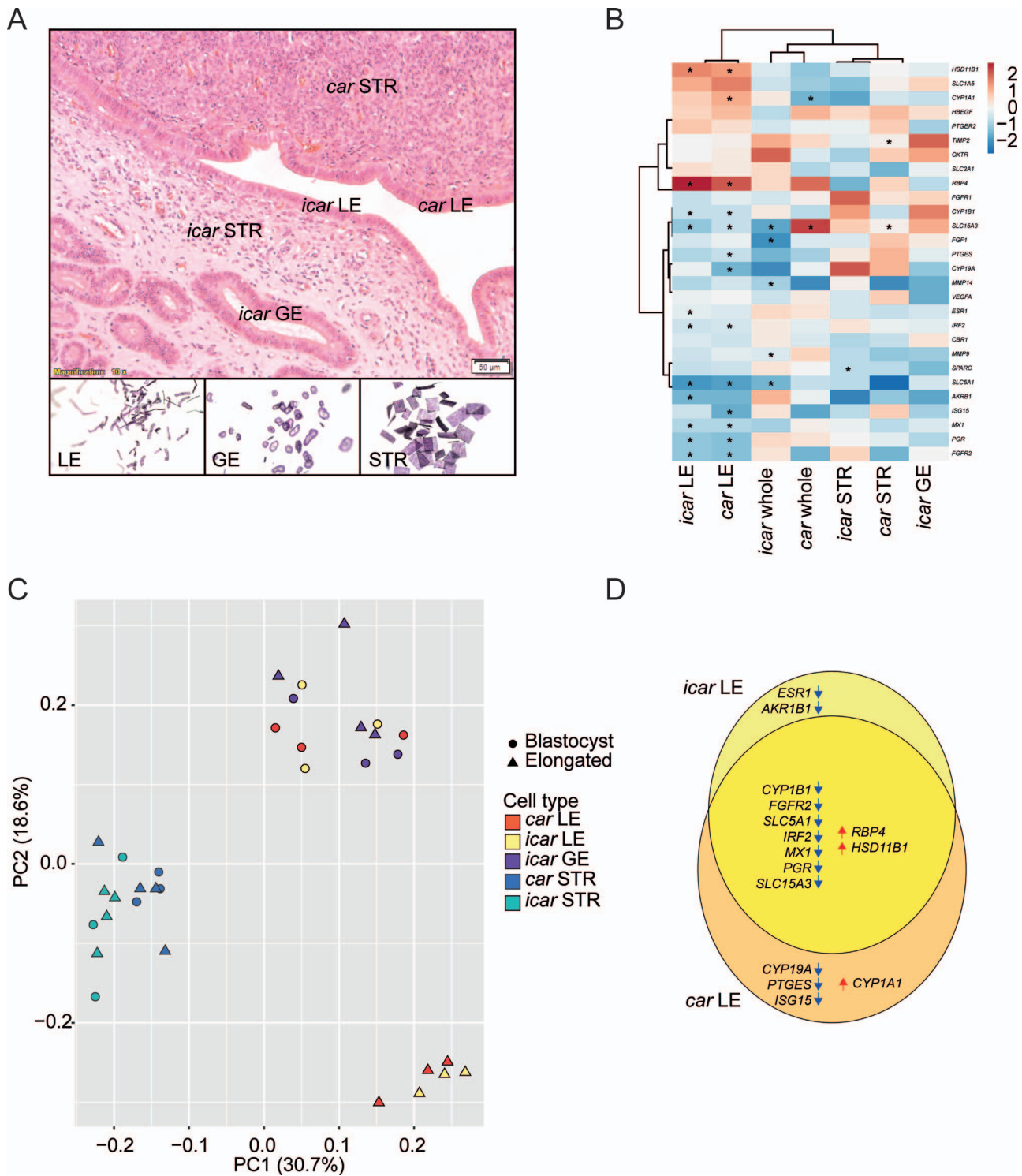
Figure 1. Cell-type–specific expression dynamics during roe deer embryo development. (A) Histological section showing the different cell types in the endometrium. Below, the respective cell types in the LMD collection caps are shown. (B) Heatmap of the log$_2$ centered complete dataset of mean fold changes between the samples corresponding to the blastocyst and elongated embryos. The star (*) displays a statistically significant difference between the two developmental stages as compared by a T-test ($P < 0.05$). The mRNA of genes higher expressed at the elongated state are shown in red, whereas those higher expressed at the blastocyst stage are shown in blue. (C) Principal component analysis (PCA) of the log$_2$ centered complete dataset. Each point represents a sample, colors indicate the different cell types, and shapes the developmental stage, i.e., circles and triangles represent endometrial samples corresponding to blastocysts and elongated embryos, respectively. The percentages indicate the explained variability by PC1 and PC2. (D) Venn diagram of all differentially expressed genes in the *icar* LE and *car* LE between the endometrium corresponding to blastocysts and elongated embryos. The gene names of the DEG are displayed in the respective parts, and blue and red arrows represent down-regulated and up-regulated genes.
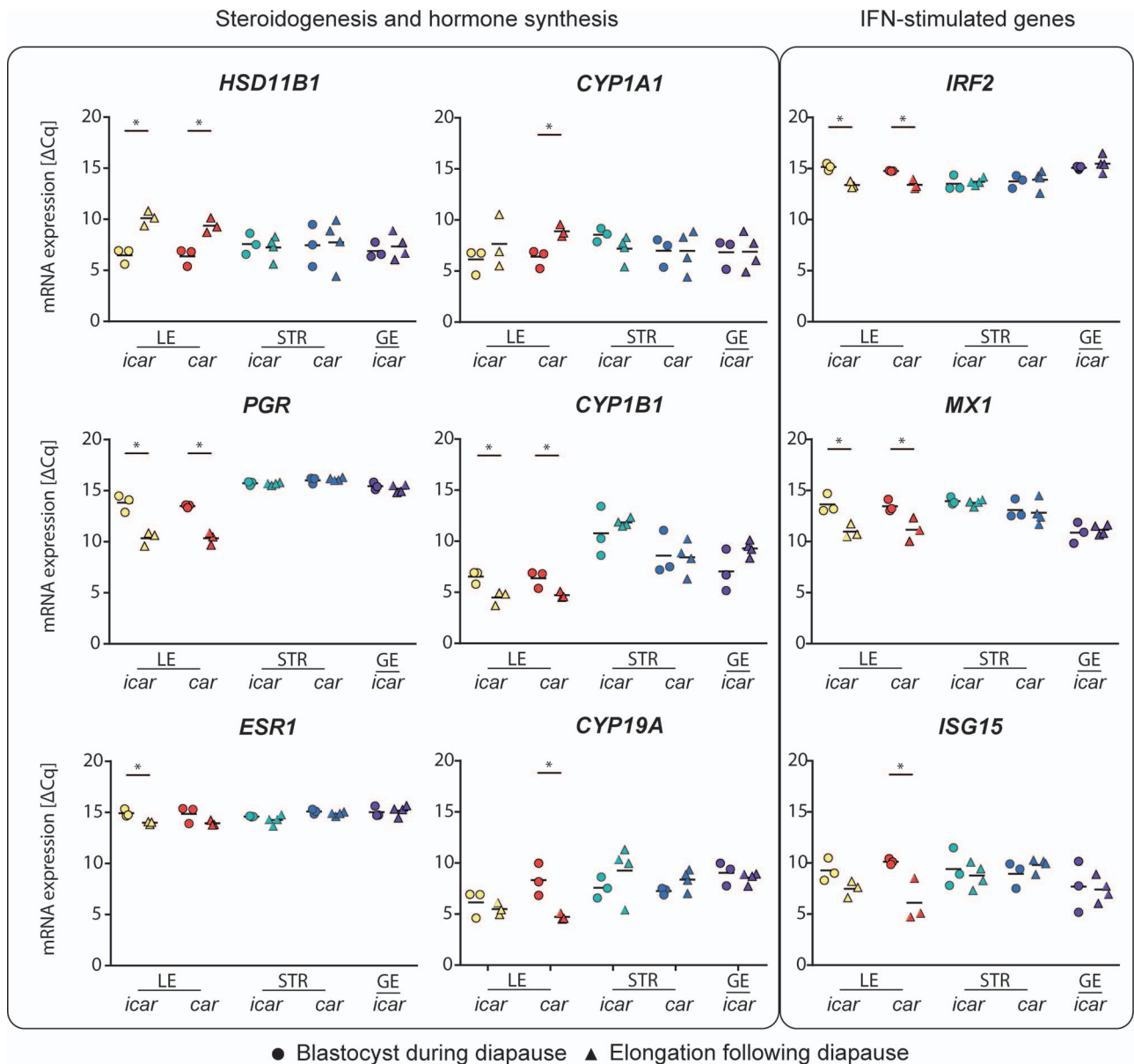
Figure 2. Gene expression of genes involved in steroidogenesis and hormone synthesis, and IFN-stimulated genes. DEG in different endometrial cell types between the developmental stages (blastocysts or elongated embryos). The normalized expression per gene is displayed for each cell type (n = 3–4). The two developmental stages are compared by a T-test, and significant differences are marked * ($P < 0.05$) accordingly.

fold, *PGR* a 11.1-fold, and *ESR1* a 1.9-fold lower expression following embryo elongation. In the *car* LE, the expression of *HSD11B1*, *CYP19A*, *CYP1A1*, *CYP1B1*, and *PGR* was significantly different during diapause and following embryo elongation (Figure 2). *HSD11B1* showed an 8.0-fold and *CYP1A1* a 5.6-fold higher expression following embryo elongation. *CYP19A*, *CYP1B1*, and *PGR* showed a 12.1-, 3.4-, and 8.9-fold lower expression following embryo elongation, respectively.

Strikingly, the expression of classical IFN-stimulated genes was significantly lower in the *icar* LE upon roe deer embryo elongation; *IRF2* (3.4-fold in *icar* and 2.5-fold in *car* LE), *MX1* (6.3-fold in *icar* and 4.9-fold in *car* LE), and *ISG15* (16.2-fold in *car* LE) (Figure 2).

The prostaglandin synthases *AKR1B1* and *PTGES* were significantly lower abundant following elongation in the *icar* and *car*

LE, respectively (Figure 3). *AKR1B1* was 17.3-fold lower expressed in the *icar* LE, whereas *PTGES* was 3.1-fold less abundant in the *car* LE.

The transporter *SLC15A3* was significantly lower expressed in the LE upon elongation (10.7-fold in *icar* and 3.1-fold in *car*), and in addition, significantly higher expressed in the *icar* GE upon elongation (3.3-fold) (Figure 3). The transporter *SLC5A1* was significantly lower expressed in the LE (42.1-fold in *icar*, and 21-fold in *car*) (Figure 3). Both genes that were involved in proliferation and tissue remodeling, i.e., *RBP4* and *FGFR2*, were differentially expressed in the *icar* and *car* LE (Figure 3). *RBP4* was higher expressed in the *icar* LE (92.4-fold) and in the *car* LE (25.8-fold), whereas *FGFR2* was lower expressed in the *icar* LE (11.1-fold) and in the *car* LE following embryo elongation (9.9-fold).
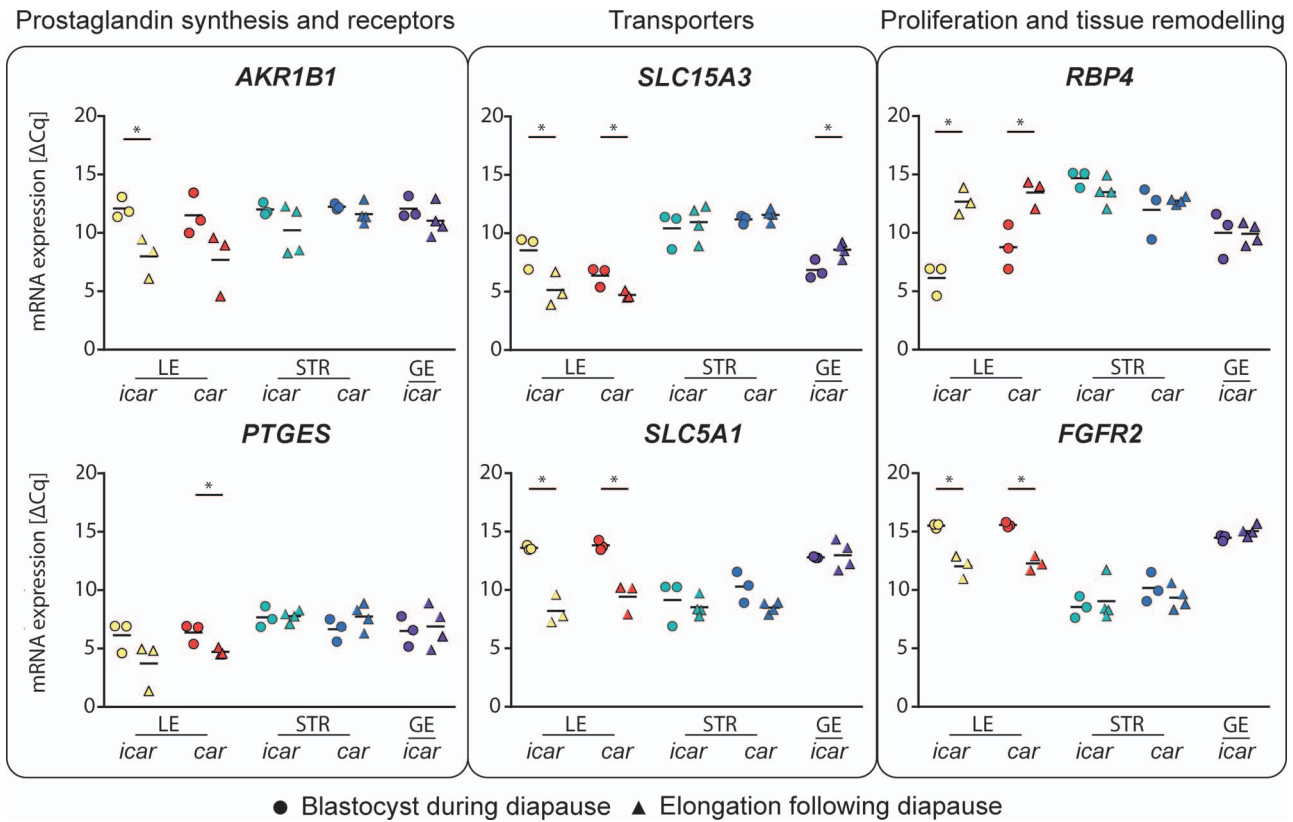
Figure 3. Gene expression of DEG in the functional categories "prostaglandin synthesis and receptors," "transporters," and "proliferation and tissue remodeling." DEG in different endometrial cell types between the developmental-stage blastocysts or elongated embryos. The normalized expression is displayed for each cell type per gene ($n = 3–4$). The two developmental stages are compared by a *T*-test, and significant differences are marked * ($P < 0.05$) accordingly.

Loss of the progesterone receptor in the luminal epithelium

Semiquantitative scoring of the PR in the LE, superficial glands, deep glands, stroma, myometrium, and vascular endothelium is shown in Table 1. The staining was nuclear and scored according to the staining intensity as "negative," "weak/sporadic," "medium," and "strong." Irrespective of embryonic developmental stage or sampling date, the PR protein was present in the vascular epithelium. In only 2 out of 19 uterine samples, a weak/sporadic LE staining was observed. The abundance in the GE, STR, and myometrium decreased over time. The staining intensity was weak/sporadic to strong until December. Only three out of eight animals displayed a weak/sporadic to strong staining intensity in these respective cell types until the end of December. Representative pictures of four animals are shown in Figure 4.

Discussion

In ruminants, embryo-derived IFNτ leads to the lack of oxytocin receptor (OXTR) up-regulation [19]. Thereby, IFNτ prevents luteolysis and facilitates MRP [19]. In cattle and sheep, the expression of IFN-stimulated genes is highly increased due to IFNτ expression by the ovoid embryo [1]. Moreover, infusion with IFNτ morpholino antisense oligonucleotides resulted in severely growth-retarded ovine conceptuses [27]. Opposing this MRP mechanism in the latter and other ruminants, a lower abundance of the classical IFN-stimulated genes *IRF2*, *MX1*, and *ISG15* was observed in the roe deer in the

presence of an elongated embryo. This finding is in line with the lack of minute amounts of IFNτ and the lack of any detected interferon in the antiviral assay [19]. Previously, it has been presumed that IFNτ accounts for the down-regulation of the ESR1 at day 16 of pregnancy in cattle [6]. We hypothesized that *ESR1* was affected differently in roe deer lacking IFNτ and that further studies investigating the role of *PGR* down-regulation might reveal novel progestamedin signaling pathways. The immunohistochemical analysis of the uterine PR protein abundance subdivided the sample set into two distinct phases, i.e., September to December 2 and December 9 until 28. This suggest a sampling date dependency, which is potentially caused by prolonged P4 exposure. A loss of PR has been suggested to support embryo development and implantation [9]. In cattle, the loss of the PR protein in the LE and GE is observed from day 12/13 of the cycle and during pregnancy [5, 6], whereas in pregnant sheep, this takes place from day 14 onward [7]. This might indicate that the loss of the LE PR in the roe deer takes place before diapause or is associated with the induction of diapause.

Our analysis allowed a novel explorative molecular analysis of cell-type-specific endometrial mRNA expression. The LE forms the initial embryo–maternal contact surface and constitutes the site for embryo implantation. These cells showed most DEG comparing the blastocyst and elongated embryo stages [28]. Both the LE and GE in sheep show a vast number of DEG between the blastocyst and elongated embryos in a developmental-stage dependent manner, i.e., from ovoid to elongated and fully elongated [3]. We suppose a likewise dynamical process in roe deer. With

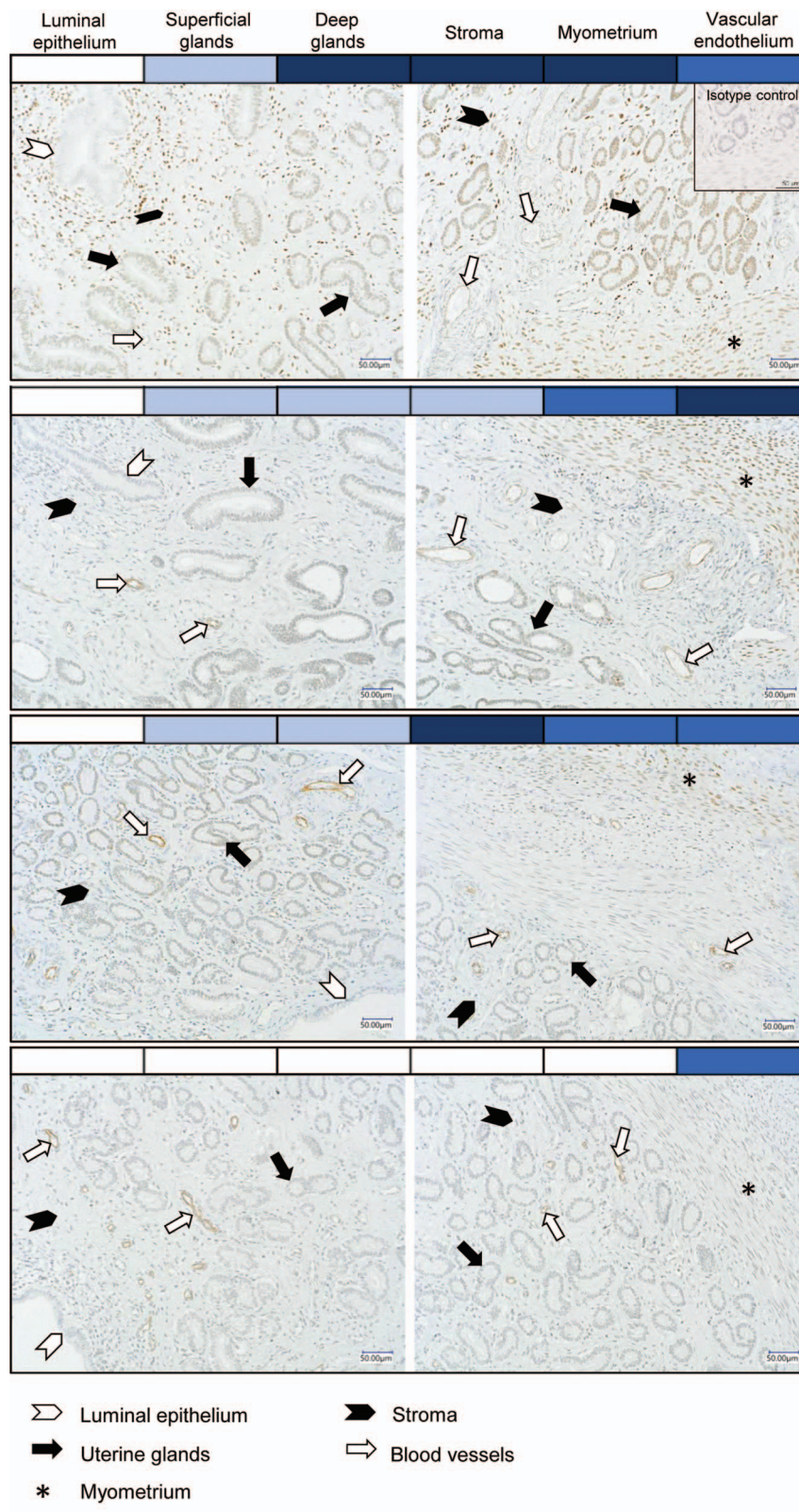**Figure 4.** Localization of the progesterone receptor (PR) by immunohistochemistry. Representative images of four different animals with various degrees of staining intensity in the luminal epithelium, superficial glands, deep glands, stroma, myometrium, and vascular endothelium. The color code ranging from white to dark blue indicates a negative, weak/sporadic, medium, and strong staining intensity.

Table 1. Semiquantitative scoring of progesterone receptor (PR) immunohistochemistry in the roe deer uterus. The color code ranging from white to dark blue indicates a negative, weak/sporadic, medium, and strong staining intensity

Date of sampling	Embryo size in mm	Luminal epithelium	Superficial glands	Deep glands	Stroma	Myometrium	Vascular endothelium
10.09.2016	0.4						
21.10.2016	0.3						
21.10.2016	0.5						
29.10.2016	0.9						
08.11.2016	0.9						
08.11.2016	1.4						
28.11.2016	4.3						
30.11.2016	1.3						
30.11.2016	1.5						
01.12.2016	1.8						
02.12.2016	26.0						
09.12.2016	2.0						
09.12.2016	1.9						
09.12.2016	52.0						
10.12.2016	1.1						
10.12.2016	1.3						
10.12.2016	2.2						
10.12.2016	60.0						
28.12.2016	1.5						

adequate more numerous samples at hand, this hypothesis may be further substantiated.

HSD11B1, *ESR1*, *PGR*, *SLC15A3* (in GE), *AKR1B1*, *SLC5A1*, and *RBP4* showed mRNA expression changes in line with previously reported changes in cattle, sheep, mice, and humans. However, the IFN-stimulated genes *IRF2*, *MX1*, *ISG15*, *PTGES*, and *FGFR2* did not follow the expected expression pattern as observed in other ruminants. The deviation in gene expression in roe deer endometrium versus other species might reflect a time-dependent and/or species-dependent effect.

The cortisone reductase *HSD11B1* was higher abundant during elongation in the LE as reported earlier in sheep, where *HSD11B1* has been shown to be involved in conceptus elongation [29]. We hypothesize that cortisone metabolism is involved in inducing and/or supporting embryo elongation. Furthermore, the slightly reduced, but relatively low, expression of aromatase *(CYP19A)* in *car* LE indicates little conversion of androgens to estrogens. Like in pigs, sheep, and cattle, both *ESR1* and, most prominently, *PGR* were lost from the LE prior to embryo implantation [1, 5, 6]. The concept of progestamedins comprises the P4-mediated stimulation of stromal cells expressing the PR resulting in the expression of proteins that accomplish the action of P4 [8]. This concept may as well hold true for the roe deer.

The prostaglandin F2α synthases *AKR1B1* and, to a lesser extent, prostaglandin E synthase (*PTGES*) transcript abundances were significantly lower in the presence of an elongated embryo. The expression of *AKR1B1* has previously been shown to be reduced prior to embryo implantation in pigs, whereas the expression of *PTGES* was found to be significantly increased [30]. The abundance of PGE$_2$ and PGF$_{2\alpha}$ has previously been shown to be significantly increased prior to and upon embryo elongation in cattle [31]. Our findings

might reflect the temporal difference in mRNA and prostaglandin abundance. Alternatively, the actual time point of prostaglandins playing a regulatory role prior to embryo elongation might have been overlooked by not including the endometrial samples of embryos right before elongation. By principle, the latter are not possible to collect at huntings.

The expression of *SLC15A3* contradicts the expression profiles in sheep and cattle, where it is interesting to note that *SLC15A3* in the *icar* GE followed the increase in expression upon elongation [1, 32]. It has previously been shown that (1) the expression of *SLC15A3*, a cotransporter of short chain peptides, which also exports histidine (His) from lysosomes [33], increased prior to bovine embryo elongation [34], and that (2) IFNτ can increase its expression [32]. It has been hypothesized that the increased expression of *SLC15A3* may provide the developing embryo with His as source for protein synthesis [32]. Even though the down-regulation of *SLC15A3* expression in the LE would contradict this hypothesis in roe deer, the increased expression in the GE would support the idea that more uterine fluid His would fulfil the embryonic amino acid demands. The apical glucose transporter *SLC5A1* has been shown to be increased in sheep following IFNτ stimulation, an effect that was diminished by infusion of a prostaglandin synthase inhibitor [35]. The lack of IFNτ in roe deer might explain the decrease in *SLC5A1* upon elongation. In addition, a gradual decrease in both mRNA and protein abundance in sheep from day 12 of pregnancy and onward has previously been reported [36], which is in line with the observed decrease in the current study. We hypothesize that a decrease in expression of *SLC5A1* takes place prior to elongation, where the embryo has an increased demand of glucose. The latter has been determined earlier in the uterine fluid of developing roe deer embryos [14].

In line with a previously reported up-regulation of *RBP4* in pigs [37], *RBP4* was found to be significantly more abundant in the roe deer endometrium at elongation than during diapause. In cattle, the intrauterine administration of IFNτ diminishes the expression of uterine RBP4 [38], potentially indicating an IFNτ-dependent RBP4 expression. In humans, *RBP4* was significantly up-regulated during decidualization of the stroma cells [39], implying an important role for *RBP4* during embryo implantation. The expression of roe deer *FGFR2* was significantly less at elongation, contradicting findings in preimplantation pig and cattle endometrium [40, 41]. Previously, the activation of *FGFR2* by FGF2 has been shown to activate the PI3K/AKT pathway. This promotes LE cell proliferation, which may enhance uterine receptivity and placentation [40]. In addition, loss of *FGFR2* in mice has been implicated in peri-implantation pregnancy loss [42], stressing its importance during the implantation process. The biological function of a down-regulation in roe deer prior to implantation remains to be elucidated.

In conclusion, our data show that the roe deer endometrium, particularly the LE, senses the presence of the elongated embryo. The low endometrial aromatase mRNA expression (*CYP19A*) is indicative of low estrogen synthesis not only during diapause but also after elongation. We propose that the uterine loss of PR as well as the presence of prostaglandins, amino acids, and RBP4 potentially play important roles in embryo elongation, the receptivity of the endometrium, as well as preparation for implantation. The roe deer offers the opportunity to further investigate the embryo–maternal interaction on a high scale time resolution by transcriptome analyses as a model that is devoid of IFNτ, and in which early embryo development is particularly slow and decoupled from embryo elongation by embryonic diapause.

Supplementary data

Supplementary data are available at *BIOLRE* online.

Acknowledgments

The samples were collected in collaboration with local hunters in Switzerland and Southern Germany. The data produced and analyzed in this paper were generated in collaboration with ScopeM and the Genetic Diversity Centre (GDC), ETH Zurich. The authors are active participants of the COST Action "CellFit" CA16119 (In vitro 3D total cell guidance and fitness).

Conflict of interest

The authors declare that there are no conflicts of interest.

Author contributions

VvdW performed sample collection, selected target genes, coordinated and conducted the experiments, analyzed the data, and wrote the manuscript. BP conducted the LMD and gene expression experiments. ARV and VM performed sample collection. CS performed and analyzed the ELISA experiments. MPK performed and analyzed the PR IHC experiment. BD coordinated the study and sampling and performed sample collection. SEU conceptualized the study, coordinated and supervised the project, and critically revised the manuscript. All authors read, edited, and approved the final manuscript.

References

1. Bazer FW. Pregnancy recognition signaling mechanisms in ruminants and pigs. *J Anim Sci Biotechnol* 2013; **4**:23.
2. Niklaus AL, Pollard JW. Mining the mouse transcriptome of receptive endometrium reveals distinct molecular signatures for the luminal and glandular epithelium. *Endocrinology* 2006; **147**:3375–3390.
3. Brooks K, Burns GW, Moraes JGN, Spencer TE. Analysis of the uterine epithelial and conceptus transcriptome and luminal fluid proteome during the peri-implantation period of pregnancy in sheep. *Biol Reprod* 2016; **95**:88.
4. Short RV, Hay MF. Delayed Implantation in the roe deer *Capreolus capreolus*. In: Rowlands IW (ed.), *Comparative Biology of Reproduction in Mammals*. New York: Academic Press; 1966: 173–194.
5. Okumu LA, Forde N, Fahey AG, Fitzpatrick E, Roche JF, Crowe MA, Lonergan P. The effect of elevated progesterone and pregnancy status on mRNA expression and localisation of progesterone and oestrogen receptors in the bovine uterus. *Reproduction* 2010; **140**:143–153.
6. Robinson RS, Mann GE, Lamming GE, Wathes DC. Expression of oxytocin, oestrogen and progesterone receptors in uterine biopsy samples throughout the oestrous cycle and early pregnancy in cows. *Reproduction* 2001; **122**:965–979.
7. Bairagi S, Grazul-Bilska AT, Borowicz PP, Reyaz A, Valkov V, Reynolds LP. Placental development during early pregnancy in sheep: Progesterone and estrogen receptor protein expression. *Theriogenology* 2018; **114**:273–284.
8. Bazer FW, Burghardt RC, Johnson GA, Spencer TE, Wu G. Interferons and progesterone for establishment and maintenance of pregnancy: interactions among novel cell signaling pathways. *Reprod Biol* 2008; **8**:179–211.
9. Bazer FW, Burghardt RC, Johnson GA, Spencer TE, Wu G. Mechanisms for the establishment and maintenance of pregnancy: Synergies from scientific collaborations. *Biol Reprod* 2018; **99**:225–241.
10. Bischoff TLW. *Die Entwicklungsgeschichte des Rehes*. Giessen, Germany: J. Bicker'sche Buchhandlung; 1854.
11. Renfree MB, Fenelon JC. The enigma of embryonic diapause. *Development* 2017; **144**:3199–3210.
12. Aitken RJ. Calcium and zinc in the endometrium and uterine flushings of the roe deer (*Capreolus capreolus*) during delayed implantation. *J Reprod Fertil* 1974; **40**:333–340.
13. Aitken RJ. Delayed implantation in roe deer (*Capreolus capreolus*). *J Reprod Fertil* 1974; **39**:225–233.
14. Aitken RJ. Uterine secretion of fructose in the roe deer. *J Reprod Fertil* 1976; **46**:439–440.
15. Rudolf Alba Vegas A, Drews B, van der Weijden VA, Milojevic V, Hankele AK, Schuler G, Ulbrich SE. Do ovarian steroid hormones control the resumption of embryonic growth following the period of diapause in roe deer (*Capreolus capreolus*)? *Reprod Biol* 2019; **19**:149–157.
16. van der Weijden VA, Bick JT, Bauersachs S, Arnold GJ, Frohlich T, Drews B, Ulbrich SE. Uterine fluid proteome changes during diapause and resumption of embryo development in roe deer. *Reproduction* 2019; **158**:13–24.
17. Lambert RT. A pregnancy-associated glycoprotein (Pag) unique to the roe deer (*Capreolus capreolus*) and its role in the termination of embryonic diapause and maternal recognition of pregnancy. *Isr J Zool* 2005; **51**:1–11.
18. Hoffmann B, Barth D, Karg H. Progesterone and estrogen levels in peripheral plasma of the pregnant and nonpregnant roe deer (*Capreolus capreolus*). *Biol Reprod* 1978; **19**:931–935.
19. Flint AP, Krzywinski A, Sempere AJ, Mauget R, Lacroix A. Luteal oxytocin and monoestry in the roe deer *Capreolus capreolus*. *J Reprod Fertil* 1994; **101**:651–656.
20. Schanzenbach CI, Bernal-Ulloa SM, van der Weijden VA, Pfaffl MW, Buttner M, Wunsch A, Ulbrich SE. Blastocysts depict sex-specific signalling of IFNT transcription, translation and activity. *Reproduction* 2018; **157**:245–258.

21. Nestorov P, Hotz HR, Liu Z, Peters AH. Dynamic expression of chromatin modifiers during developmental transitions in mouse preimplantation embryos. *Sci Rep* 2015; **5**:14347.

22. van der Weijden VA, Chen S, Bauersachs S, Ulbrich SE, Schoen J. Gene expression of bovine embryos developing at the air-liquid interface on oviductal epithelial cells (ALI-BOEC). *Reprod Biol Endocrinol* 2017; **15**:91.

23. Kowalewski MP, Schuler G, Taubert A, Engel E, Hoffmann B. Expression of cyclooxygenase 1 and 2 in the canine corpus luteum during diestrus. *Theriogenology* 2006; **66**:1423–1430.

24. Mariusz Pawel K, Hakki Bülent B, Christiane P, Selim A, Hans K, Ibrahim K, Bernd H. Canine placenta: a source of prepartal prostaglandins during normal and antiprogestin-induced parturition. *Reproduction* 2010; **139**:655–664.

25. Vandesompele J, De Preter K, Pattyn F, Poppe B, Van Roy N, De Paepe A, Speleman F. Accurate normalization of real-time quantitative RT-PCR data by geometric averaging of multiple internal control genes. *Genome Biol* 2002; **3**: Research0034.

26. Wickham H. *ggplot2: Elegant Graphics for Data Analysis*. New York: Springer-Verlag; 2016.

27. Brooks K, Spencer TE. Biological roles of interferon tau (IFNT) and type I IFN receptors in elongation of the ovine conceptus. *Biol Reprod* 2015; **92**:47.

28. Gray CA, Bartol FF, Tarleton BJ, Wiley AA, Johnson GA, Bazer FW, Spencer TE. Developmental biology of uterine glands. *Biol Reprod* 2001; **65**:1311–1323.

29. Brooks K, Burns G, Spencer TE. Biological roles of hydroxysteroid (11-beta) dehydrogenase 1 (HSD11B1), HSD11B2, and glucocorticoid receptor (NR3C1) in sheep conceptus elongation. *Biol Reprod* 2015; **93**:38.

30. Seo H, Choi Y, Shim J, Yoo I, Ka H. Comprehensive analysis of prostaglandin metabolic enzyme expression during pregnancy and the characterization of AKR1B1 as a prostaglandin F synthase at the maternal-conceptus interface in pigs. *Biol Reprod* 2014; **90**:99.

31. Ulbrich SE, Schulke K, Groebner AE, Reichenbach HD, Angioni C, Geisslinger G, Meyer HH. Quantitative characterization of prostaglandins in the uterus of early pregnant cattle. *Reproduction* 2009; **138**:371–382.

32. Groebner AE, Rubio-Aliaga I, Schulke K, Reichenbach HD, Daniel H, Wolf E, Meyer HH, Ulbrich SE. Increase of essential amino acids in the bovine uterine lumen during preimplantation development. *Reproduction* 2011; **141**:685–695.

33. Daniel H, Kottra G. The proton oligopeptide cotransporter family SLC15 in physiology and pharmacology. *Pflugers Arch* 2004; **447**:610–618.

34. Klein C, Bauersachs S, Ulbrich SE, Einspanier R, Meyer HH, Schmidt SE, Reichenbach HD, Vermehren M, Sinowatz F, Blum H, Wolf E. Monozygotic twin model reveals novel embryo-induced transcriptome changes of bovine endometrium in the preattachment period. *Biol Reprod* 2006; **74**:253–264.

35. Dorniak P, Bazer FW, Spencer TE. Prostaglandins regulate conceptus elongation and mediate effects of interferon tau on the ovine uterine endometrium. *Biol Reprod* 2011; **84**:1119–1127.

36. Gao H, Wu G, Spencer TE, Johnson GA, Bazer FW. Select nutrients in the ovine uterine lumen. II. Glucose transporters in the uterus and peri-implantation conceptuses. *Biol Reprod* 2009; **80**:94–104.

37. Wang L, Zhang L, Li Y, Li W, Luo W, Cheng D, Yan H, Ma X, Liu X, Song X, Liang J, Zhao K et al. Data mining in networks of differentially expressed genes during sow pregnancy. *Int J Biol Sci* 2012; **8**:548–560.

38. Godkin JD, Smith SE, Johnson RD, Dore JJ. The role of trophoblast interferons in the maintenance of early pregnancy in ruminants. *Am J Reprod Immunol* 1997; **37**:137–143.

39. Pavone ME, Malpani S, Dyson M, Bulun SE. Altered retinoid signaling compromises decidualization in human endometriotic stromal cells. *Reproduction* 2017; **154**:107–116.

40. Lim W, Bae H, Bazer FW, Song G. Stimulatory effects of fibroblast growth factor 2 on proliferation and migration of uterine luminal epithelial cells during early pregnancy. *Biol Reprod* 2017; **96**:185–198.

41. Okumu LA, Forde N, Mamo S, McGettigan P, Mehta JP, Roche JF, Lonergan P. Temporal regulation of fibroblast growth factors and their receptors in the endometrium and conceptus during the pre-implantation period of pregnancy in cattle. *Reproduction* 2014; **147**:825–834.

42. Filant J, DeMayo FJ, Pru JK, Lydon JP, Spencer TE. Fibroblast growth factor receptor two (FGFR2) regulates uterine epithelial integrity and fertility in mice. *Biol Reprod* 2014; **90**:7.